AD-A079 587 AIR FORCE TECHNICAL APPLICATIONS CENTER PATRICK AFB FL F/G 18/11
INTEGRAL EQUATION SPACE-ENERGY FLUX SYNTHESIS FOR SPHERICAL SYS--ETC(U)
NOV 79 E W SKLUZACEK

UNCLASSIFIED AFTAC-TR-79-69 NL

| OF |
AD
A079587

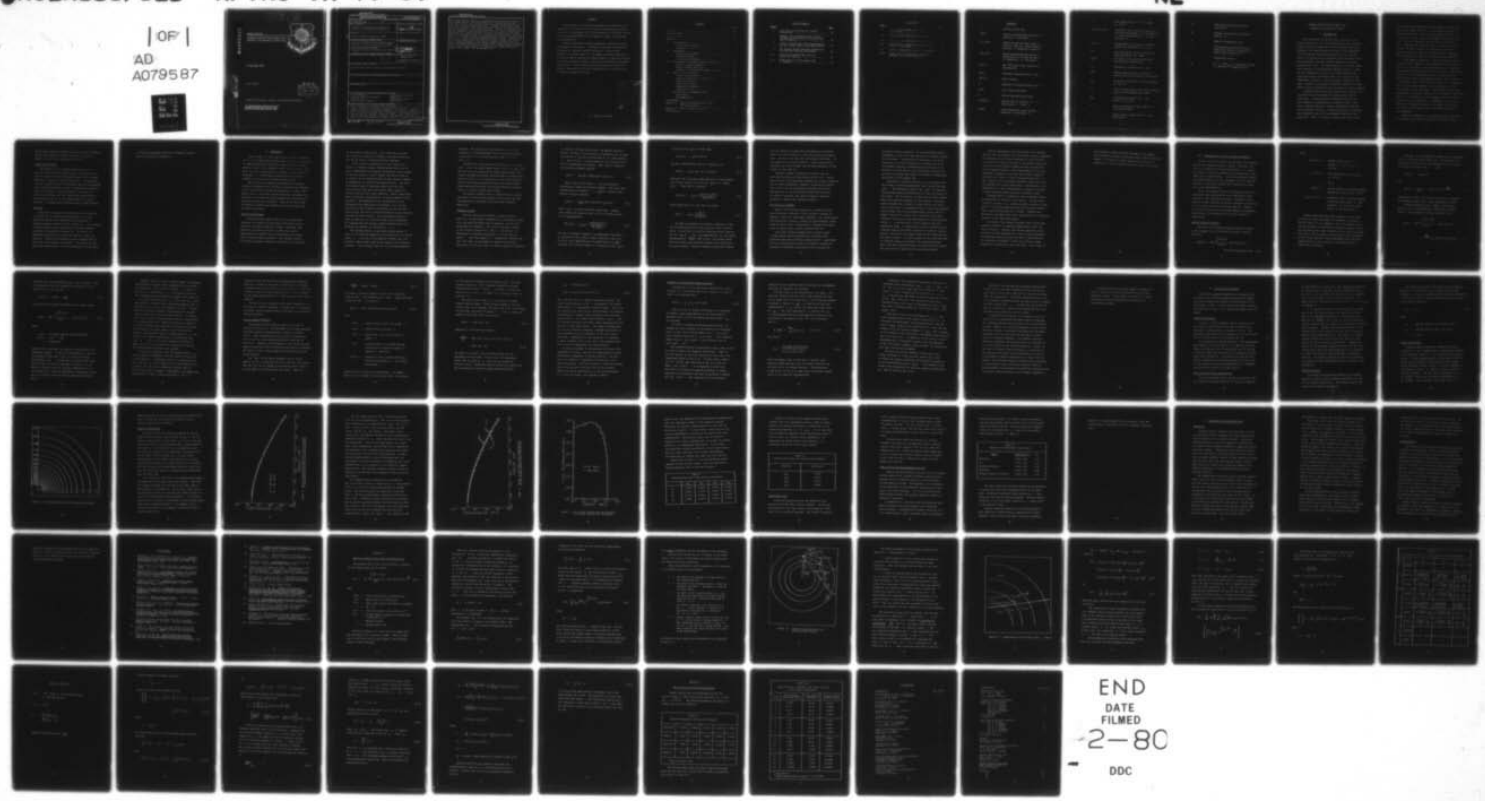

END
DATE
FILMED
2-80
DDC

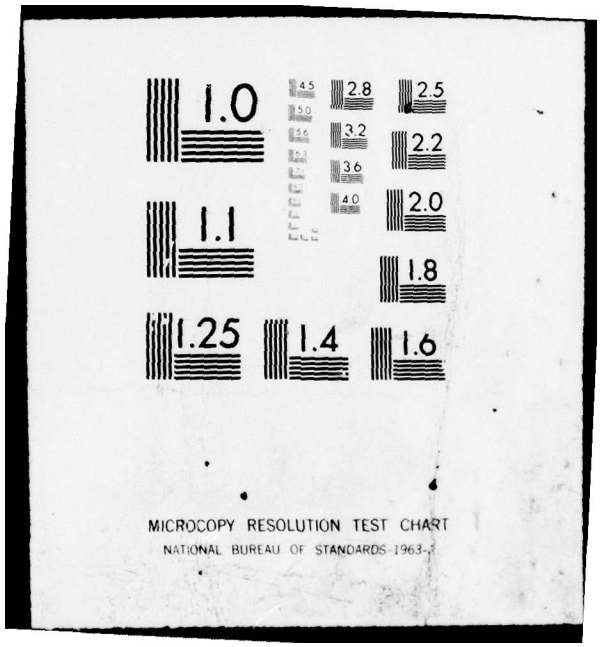
1.0
1.1
1.25
1.4
1.6
1.8
2.0
2.2
2.5
2.8
3.2
3.6
4.0
4.5
5.0
5.6
6.3
MICROCOPY RESOLUTION TEST CHART
NATIONAL BUREAU OF STANDARDS-1963-A

AFTAC-TR-79-69

INTEGRAL EQUATION SPACE-ENERGY FLUX SYNTHESIS FOR SPHERICAL SYSTEMS (U)

21 NOVEMBER 1979

Final Report

Approved for public release; distribution unlimited.

AIR FORCE TECHNICAL APPLICATIONS CENTER
HEADQUARTERS UNITED STATES AIR FORCE
PATRICK AIR FORCE BASE, FLORIDA 32925

UNCLASSIFIED

SECURITY CLASSIFICATION OF THIS PAGE *(When Data Entered)*

REPORT DOCUMENTATION PAGE		READ INSTRUCTIONS BEFORE COMPLETING FORM
1. REPORT NUMBER AFTAC-TR-79-69	2. GOVT ACCESSION NO.	3. RECIPIENT'S CATALOG NUMBER
4. TITLE *(and Subtitle)* Integral Equation Space-Energy Flux Synthesis for Spherical Systems		5. TYPE OF REPORT & PERIOD COVERED Final Report 6. PERFORMING ORG. REPORT NUMBER
7. AUTHOR(s) Eugene W. Skluzacek, Major, USAF		8. CONTRACT OR GRANT NUMBER(s) 013 050
9. PERFORMING ORGANIZATION NAME AND ADDRESS Air Force Technical Applications Center Patrick Air Force Base, Florida 32925		10. PROGRAM ELEMENT, PROJECT, TASK AREA & WORK UNIT NUMBERS
11. CONTROLLING OFFICE NAME AND ADDRESS Air Force Technical Applications Center/TRE Patrick Air Force Base, Florida 32925		12. REPORT DATE 21 November 1979 13. NUMBER OF PAGES 79
14. MONITORING AGENCY NAME & ADDRESS *(if different from Controlling Office)*		15. SECURITY CLASS. *(of this report)* UNCLASSIFIED 15a. DECLASSIFICATION/DOWNGRADING SCHEDULE

16. DISTRIBUTION STATEMENT *(of this Report)*

Approved for public release; distribution unlimited.

17. DISTRIBUTION STATEMENT *(of the abstract entered in Block 20, if different from Report)*

18. SUPPLEMENTARY NOTES

19. KEY WORDS *(Continue on reverse side if necessary and identify by block number)*

Flux Synthesis	Supercritical Systems
Integral Transport Equation	Neutronics
Neutron Flux	Jezebel Calculation
Space-Energy Synthesis	Rossi Alpha

20. ABSTRACT *(Continue on reverse side if necessary and identify by block number)*

The calculation of neutron flux distribution and growth rate for small, spherically symmetric systems usually requires extensive computing time on the largest machines. To minimize computing time, a compromise between the simplicity of diffusion theory and the accuracy of transport theory is needed. The Serber-Wilson method, Feynman's method, and early flux synthesis methods are used as the foundation for integral equation synthesis (IES) which

(continued)

DD FORM 1 JAN 73 1473

013 050 i

UNCLASSIFIED

SECURITY CLASSIFICATION OF THIS PAGE *(When Data Entered)*

is an approximate, numerical technique for obtaining the spatial and energy neutron flux distributions in multiplying systems. In IES, the integral form of the neutron transport equation is specialized to spatial dependence only, and then solved numerically for the two lowest order eigenfunctions. Similar specialization to energy dependence only yields a second set of trial eigenfunctions. Using standard perturbation methods, the two sets of trial eigenfunctions are synthesized into a single, two-dimensional solution. The IES technique was used to calculate the flux and multiplication factor, k, of the critical plutonium sphere, Jezebel. Results for k agreed to within 0.01% of published values, whereas the spatial flux, when normalized at the center, agreed to within 8% at the outer assembly boundary. The Jezebel calculation using IES required about 90 seconds CPU time on an IBM 360/75. Highly sophisticated codes require approximately 10 minutes of CDC 7600 CPU time to compute the Jezebel flux and growth rate.

Preface

This document was originally prepared as a dissertation and submitted to the faculty of the School of Engineering, Air Force Institute of Technology (AFIT), Air University, in partial fulfillment of the requirements for the degree of Doctor of Philosophy (AFIT/DS/PH/79-2).

Several individuals provided significant assistance during the course of this effort. Gratitude is extended to Mister Eric Reinhardt for computer support assistance. Doctors Henry Sandmeier and Gordon Hansen of Los Alamos Scientific Laboratory and Doctors Walter Webster and James Ferguson of Lawrence Livermore Laboratory provided interest, advice, and encouragement throughout this project. Special appreciation must be given to Major Guy Spitale, formerly of AFIT, Major George Nickel of AFIT who acted as advisors during this effort.

Contents

	Page
Preface	iii
List of Figures	v
List of Tables	vi
Notation	vii
I. Introduction	1
Purpose and Criteria	3
Overview	3
II. Background	5
Serber-Wilson Method	5
Feynman's Method	7
Flux Synthesis Methods	10
III. Development of Integral Equation Synthesis	14
Spatial Integral Equation	14
Energy Integral Equation	19
Synthesis of Spatial and Energy Solutions	23
IV. Results and Discussion	28
Jezebel Calculations	28
Cross Sections Used in Calculations	28
Numerical Details	29
Growth Rate Results	30
Computed Flux Results	32
Computation Times	38
V. Conclusions and Recommendations	42
Conclusions	42
Recommendations	44
Bibliography	46
Appendix A: Numerical Methods Used in the IES Calculations	49
Appendix B: Data Listing for Jezebel Calculations	65
Distribution	67

List of Figures

Figure		Page
1	Self-Similar Mesh Used for Jezebel Calculation.....	31
2	Spatial Flux Distribution for Jezebel Assembly as Calculated by the LASL Code and IES Method.....	33
3	Effect of Additional Trial Eigenfunction on the Jezebel Spatial Flux Distribution..	35
4	The Jezebel Energy Spectrum Computed by the LASL Code and the IES Method.....	36
A-1	Several Integration Rays and the Associated Indices.....	52
A-2	Relationship of Flux Indices and ρ Indices.....	54

List of Tables

Table		Page
I	Transformation Matrix from Jezebel Calculation.....	37
II	Mixing Coefficients for Jezebel Flux Synthesis.....	38
III	Comparison of Calculated Alpha Values.....	40
A-I	Interpolation Coefficients for a Self-Similar Radial Mesh.....	58
B-I	Gaussian Quadrature Abscissas and Weights.	65
B-II	Group Structure, Velocities and Cross Sections for Jezebel Calculation.....	66

Notation

α	neutron growth rate
$A(\vec{x},v)$	density of absorptions of neutrons at position $\vec{x}$ and speed v
$S(v'\rightarrow v)dv$	number of neutrons that emerge in velocity range dv when a neutron of velocity v' undergoes a collision
$P(\vec{x}'\rightarrow x,v)$	kernel representing the density of abosrptions at $\vec{x}$ when one neutron is released at $\vec{x}'$ with speed v
$\psi_n(x,v)$	the n^{th} order scalar neutron flux eigenfunction
$k_n(v)$	eigenvalue associated with $\psi_n(\vec{x},v)$
$\delta(\vec{x}'-\vec{x})$	delta function
B	buckling of diffusion theory solution
$\phi_n(E)$	trial energy functions
k	neutron multiplication factor
$\Phi(\vec{r},\vec{\Omega},E,t)$	neutron flux at position $\vec{r}$, energy E solid angle Ω , time t
$\Sigma(\vec{r},E)$	total macroscopic cross section at position $\vec{r}$ and energy E

ρ	path length from $\vec{r}'$ to $\vec{r}$ equal to $\lvert\vec{r}-\vec{r}'\rvert$
$f_{r'}(E'\to E;\Omega'\to\Omega)$	probability that a neutron entering a collision with energy E' and direction Ω' will emerge with energy E and direction Ω
$c(r',E')$	average number of secondary neutrons emitted per collision at (r',E')
Σ^*	total macroscopic cross section with time absorption α/v added
$\psi_n(r)$	n^{th} order of one group spatial flux distribution eigenfunction
λ_n	eigenvalue associated with $\psi_n(r)$
$n(E)$	neutron number density in units of neutrons per unit volume per unit energy
a_{ij}	expansion coefficients of trial function ψ_i and n_j
X_1	result of operating on the trial solution $\psi_1 n_1$ with two-dimensional kernel
A_{mn}	transformation matrix from $\psi_i n_j$ basis to X_m basis
ϵ	ratio of successive shell radii in a self-similar mesh
θ	angle between radius vector $\vec{r}$ and path length ρ

μ_k	direction cosines for Gaussian quadratures
w_k	weights associated with direction cosines μ_k
K	number of integration rays
C	interpolation coefficients used to express the flux as a function of ρ rather than a function of r
T	transmission factor
η_k	cos θ where θ is the angle between r_i and the k^{th} integration ray

INTEGRAL EQUATION SPACE-ENERGY FLUX SYNTHESIS FOR SPHERICAL SYSTEMS

I. Introduction

The calculations of neutron flux distributions and neutron growth rate (α) for multiplying systems currently require extensive computing time on the largest machines. Because of the immense amount of detail in the dependence of cross sections on neutron energy for fissile nuclei, there is no possibility of obtaining exact solutions to the energy-dependent neutron transport equation for general problems (Ref 2:48). The usual approach is to obtain numerical solutions to the Boltzmann transport equation. Even for one-dimensional systems, this integro-differential equation expresses the neutron flux as a function of four independent variables: position, energy, direction, and time. Accurate calculations of neutron transport are often made by finite differencing the first three of these variables.

A typical neutron transport problem might involve tens of spatial cells and perhaps ten energy groups and ten directions. Differencing this problem then results in a mesh composed of approximately a thousand "cells;" each with a specified position, energy, and neutron direction. The calculation, however, is entirely nonlocal in the sense that neutrons in any cell can influence neutrons in any other cell. Thus, to compute a neutron flux value in one

cell requires the calculation of interactions between that cell and the other 999 cells. For a typical problem of a thousand cells then, about a million interactions must be calculated in order to specify the neutron flux for a given time. In a time dependent problem, these calculations must be repeated each time the clock is advanced one step. Clearly, the usual approach to numerically solving the Boltzmann transport equation requires extensive computing time in addition to extensive computer storage capability.

If all spatial dimensions of the system under consideration are large compared to the applicable neutron mean free paths, it is possible to use diffusion theory to calculate the neutron flux and growth rate for the system. Well known because of its wide applicability, this method fails to describe many interesting problems because diffusion theory is completely local in the sense that each cell is influenced only by its nearest neighbors. One consequence of this local nature is that the shape of the spatial neutron flux distribution is strongly influenced by the boundary conditions. However, it is precisely at the boundary that this solution technique is most inaccurate. For spherical systems with a radius of a few mean free paths, all points in the system are "close" to the boundary and thus diffusion theory is not applicable.

Clearly, a compromise is needed between the simplicity of diffusion theory and the accuracy of transport theory.

An efficient solution technique that can be used on small or medium sized computers would be of value in parametric studies of small, fast, supercritical systems.

Purpose and Criteria

The purpose of the research reported here was to develop a technique that can be used to efficiently calculate the neutron flux and the neutron growth rate in small spherically symmetric, multiplying systems. The technique is to be a numerical one that maximizes the use of analytical tools and approximations in order to minimize the numerical effort and expense. Extreme accuracy is sacrificed in favor of efficiency, but the strength and significance of the technique will lie in its applicability to nonlocal problems -- problems which diffusion theory cannot describe.

Overview

This report contains five sections and two appendices. In Section II, the theoretical background of some semi-analytical methods that influenced the development of integral equation synthesis (IES) is discussed. The extension of these methods and the derivation of integral equation synthesis is presented in Section III. In Section IV, benchmark calculations are described and the results are analyzed. Finally, the conclusions and recommendations of this study are presented in Section V. In Appendix A, the numerical methods used in the IES calculations are described.

A listing of pertinent data used in benchmark calculations is presented in Appendix B.

II. Background

Early attempts to solve the neutron transport equation were based on approximations that allowed analytical solutions. As computing machinery evolved to larger and faster models, numerical methods also evolved to brute force solutions with fewer and fewer approximations. However, many of the early techniques were surprisingly accurate and can be easily extended to describe very complex problems today.

The discussion of methods and techniques of neutron transport included in this section is certainly not intended to be a comprehensive survey of such methods. Rather, the purpose here is to briefly review only those techniques that provided a foundation for and influenced the development of integral equation flux synthesis. Some of the basic ideas of synthesis methods were detailed over three decades ago by Serber and Wilson.

Serber-Wilson Method

The Serber-Wilson method (Ref 19) is an approximate technique for finding critical masses and multiplication rates for two-media, spherical systems. Developed independently by Serber and Wilson in 1945, this method approximates the neutron flux in each medium with asymptotic diffusion theory solutions. The integral form of the neutron transport equation is required to be satisfied

at the center of the system. This requirement provides the constraint necessary to define a matching coefficient for the two pieces of diffusion theory solutions.

If the system is divided into a core region and a tamper or reflector region, then diffusion theory can be used to approximate the neturon distribution in each region. In the core region or active region, the neutron density is taken to be of sinusoidal form; in the reflector region, an exponential is used for the neutron density. The true distribution shows a transition effect near the core-reflector interface where the density drops rapidly in passing from the core to the reflector. Serber represented this by allowing a discontinuity in neutron density at the interface. The magnitude of the discontinuity can be determined from conservation of neutrons; in a critical assembly the rate of neutron production in the core must exactly equal the rate of neutron absorption in the reflector (assumed infinitely thick). Once the neutron density is fixed in this way, the critical radius can be determined by requiring that the integral equation which governs the diffusion of neutrons be satisfied at $r = 0$.

The striking feature of the Serber-Wilson method is that, in the resulting equation to be solved for the critical radius, R , one side of the equation contains only core constants and the other side of the equation only reflector constants. This obviously leads to a very simple graphical

solution. The extension of the method to non-critical assemblies is straightforward since a multiplying system is equivalent to a critical one with time absorption (Ref 8:78).

Deficiencies in the Serber-Wilson approach are three-fold: first, the method cannot handle systems so small that the diffusion approximation introduces unacceptable error; second, although the method can be extended to handle three material systems, it is difficult to treat multi-material systems with varying densities; third, the method cannot easily describe the effect of the distribution of neutron energies in finite systems (Ref 6:275).

In Feynman's method, which is described next, special attention is paid to those problems arising from the fact that neutrons of different velocities have different properties.

Feynman's Method

Like the Serber-Wilson method, Feynman's method (Ref 8) is an approximate technique for calculating critical sizes and multiplication rates of spherical, active cores surrounded by reflectors. The basis of Feynman's method is the integral equation for $A(\vec{x},v)$, the density of absorptions of neutrons at position $\vec{x}$ in the core, at speed v, per unit range of v. Feynman also defines the term $S(v' \rightarrow v)dv$ as the number of neutrons (isotropic) that emerge in velcoity range dv when a neutron of velocity

v' makes a collision in the core. He further defines a kernel $P(\vec{x}' \to \vec{x}, v)$ as the density of absorptions at $\vec{x}$ when one neutron is released isotropically at $\vec{x}'$ with velocity v. The variable v merely specifies the constants to be used in calculating this kernel. Then $A(\vec{x}, v)$ satisfies the following integral equation

$$A(\vec{x}, v) = \int d\vec{x}' \int dv' \, P(\vec{x}' \to \vec{x}, v) S(v' \to v) A(\vec{x}', v') \tag{2.1}$$

Now a form for the kernel P can be obtained by considering a simple one-velocity problem. The scalar flux eigenfunctions at velocity v, $\psi_n(\vec{x}, v)$ satisfy a one-velocity integral equation

$$\psi_n(\vec{x}, v) = \frac{1}{k_n(v)} \int d\vec{x}' \, [P(\vec{x}' \to \vec{x}, v) \, \psi_n(\vec{x}', v)] \tag{2.2}$$

where $k_n(v)$ are the associated eigenvalues. Feynman then expands the kernel of Eqn (2.2) as a bilinear series of its eigenfunctions.

$$P(\vec{x}' \to \vec{x}, v) = \sum_n k_n(v) \, \frac{\psi_n(\vec{x}, v) \psi_n(\vec{x}', v)}{\int d\vec{x} \, \psi_n^2(\vec{x}, v)} \tag{2.3}$$

The crux of Feynman's method is to approximate the kernel P in various ways that allow a simple solution to Eqn (2.1). The first lower approximation (so named because it underestimates the critical radius) is to replace all the $k_n(v)$

in Eqn (2.3) by $k_o(v)$ so that then

$$P(\vec{x}' \rightarrow \vec{x}, v) = k_o(v)\ \delta(\vec{x}' - \vec{x}) \tag{2.4}$$

and after substitution, Eqn (2.1) simplifies to

$$A(\vec{x}, v) = k_o(v) \int dv'\ S(v' \rightarrow v)\ A(\vec{x}, v') \tag{2.5}$$

Similarly the first upper approximation (it overestimates the critical radius) is to set all $k_n(v) = 0$ except $k_o(v)$. Then Eqn (2.3) becomes

$$P(\vec{x}' \rightarrow \vec{x}, v) = k_o(v)\ \frac{\psi_o(\vec{x}', v)\ \psi_o(\vec{x}, v)}{\int d\vec{x}\ \psi_o^2(x, v)} \tag{2.6}$$

Substituting Eqn (2.6) into Eqn (2.1) gives

$$A(\vec{x}, v) = k_o(v)\ \frac{\psi_o(\vec{x}, v)}{\int dx\ \psi_o^2(\vec{x}, v)} \tag{2.7}$$

An implicit assumption of Feynman's approach is that the one-group problem has been solved for every velocity group. In practice, he used the diffusion theory solution for the $\psi_n(x,v)$, i.e., the eigenfunction ψ_o was always approximated by $\frac{\sin Br}{r}$ (Ref 9:163). The method itself does not require any particular approach for solving the one-group problem. However, Feynman's method does require

that the spherical system under consideration be divided into a core and a reflector, each with homogeneous composition. If this is not the case, the method breaks down. If the composition is nearly uniform, a clumsy perturbation treatment can still be made, but the main advantages of the method are lost (Ref 8).

Clearly, Feynman's method gives insight into an efficient technique for determining neutron flux. Rather than solving a two-dimensional problem (one spatial dimension and one energy dimension), Feynman's approximation allows one to solve two one-dimensional problems successively. Although this is strictly possible only when the kernel is actually separable, the idea of Feynman's method is analogous to modern flux synthesis methods.

Flux Synthesis Methods

Modern flux synthesis methods are attempts to solve multidimensional problems by first solving a sequence of simpler, usually one dimensional problems. The reconstructed multidimensional solution, although an approximation, often contains detail which is impossible or economically impractical to achieve with a direct solution (Ref 20).

Early flux synthesis methods were directed toward solving complex reactor problems and invariably used diffusion equations and thermal energy spectra. Lancefield (Ref 13) extended space-energy flux synthesis methods by avoiding the diffusion approximation and retaining the

governing transport equation. He also introduced several refinements to the basic space-energy flux synthesis method. These included: leaving both the space/angle and energy dependence of the trial function to be determined by the variational principle, incorporating discontinuous trial functions, and the use of a new variational principle for criticality problems that leads to estimates of homogeneous functionals of the unknown flux.

Lancefield's approach, however, is still plagued with the problem of choosing appropriate trial energy functions, $\phi_n(E)$. One customarily chooses the $\phi_n(E)$ to represent infinite-media spectra characteristic of the sub-regions of the system. But this choice is restricted to large systems where such solutions dominate in some regions. For small, highly enriched fuel systems, it seems likely that such a choice would lead to considerable errors in both the computed reaction rates and the calculated energy spectra (Ref 21). Indeed, Lancefield's results for a two region (core and reflector) fast reactor gave good results for multiplication factor, k , but the errors in the reflector flux were intolerably large. To reduce these errors, Lancefield used different spectra and weight functions in different regions. However, the spectra and weight functions were obtained from the known solution. To avoid reliance on the known solution, an iterative scheme was devised, but Lancefield himself admits the whole procedure became so complicated and lengthy that any practical applicability became questionable.

Nearly simultaneous with Lancefield's work, Neuhold and Ott (Ref 16) improved the space-energy synthesis approach by employing reaction rate weighting, by using realistic trial functions, and by deriving a more general analytical solution for the synthesis equations which includes the use of complex buckling. These improvements led to error reductions (compared to previous space-energy synthesis versions) of a factor of 100 in multiplication rate, k, and a factor of 20 in integral quantities sensitive to the non-separability of space and energy. Unfortunately, the applicability of these improvements is limited to systems in which diffusion theory provides an adequate model.

Cockayne (Ref 4) extended the work of Neuhold and Ott by examining the choice of trial spectra. He found that "realized" spectra, i.e., spectra actually existing at some point in the system, generally gave more accurate results than a spectrum averaged over a region. Cockayne also developed a procedure that allows calculation of a "realized" spectrum in any transition region.

In summary, flux synthesis methods offer considerable potential relative to reducing computational effort for reactor analysis. However, the various approaches suffer from lack of wide applicability. Most of these approaches are based on diffusion theory and thus the applicability is restricted to problems in which the system is large compared to the operative mean free paths. Other forms of

flux synthesis require accurate knowledge of the energy spectrum which can only be obtained through complex iterative schemes. The concept of space-energy flux synthesis is fundamental to the new method described in the next section.

III. Development of Integral Equation Synthesis

In this section we develop the equations that comprise the integral equation synthesis method. Basically, the goal is to expand the two dimensional flux, i.e., radius and energy, in terms of products of one dimensional, separated, trial eigenfunctions. The one dimensional problems are computationally easy and economical to solve, and the accuracy of the final solution can be adjusted by using more trial eigenfunctions.

First, the integral form of the transport equation is specialized and simplified for a one dimensional, monoenergetic, time independent problem. Analogous to this spatial integral equation and based on neutron conservation, we next develop the energy integral equation. Finally, the synthesis procedure is described whereby the expansion coefficients are determined and the final solution is constructed.

Spatial Integral Equation

The basis of the integral equation synthesis method is the integral form of the neutron transport equation (Ref 6:27)

$$\Phi(\vec{r},\vec{\Omega},E,t) = \int dV' \frac{e^{-\int_0^{\rho} \Sigma(E,\rho')d\rho'}}{4\pi|\vec{r}-\vec{r}'|^2} \int dE' \, \Phi(\vec{r}',\vec{\Omega}',E',t') \Sigma(\vec{r}',E')C(r',E')f_{r'}(E'\rightarrow E;\ \Omega'\rightarrow\Omega) \qquad (3.1)$$

where

$\Phi(\vec{r},\Omega,E,t)$ = neutron flux at point $\vec{r}$, energy E, solid angle Ω, at time t

$\Sigma(r',E')$ = total macroscopic cross section at $(\vec{r}',E')$

ρ = $|\vec{r}-\vec{r}'|$

$C(\vec{r}',E')$ = average number of secondary neutrons emitted per collision at $(\vec{r}',E')$

$f_{r'}(E'\rightarrow E;\Omega'\rightarrow\Omega)$ = probability that a neutron entering a collision with energy E' and direction Ω' will emerge with energy E and direction Ω.

Several simplifications and assumptions are now made in order to reduce the number of independent variables in the flux that is to be computed. First, the angular variation of the flux is eliminated by assuming isotropic scatter and integrating both sides of Eqn (3.1) over all solid angle. From now on, the all angle or scalar flux is being computed. It will become apparent in the development below that this simplification is not essential to the method, but is a significant convenience.

Secondly, the time dependent problem can be transformed into a stationary problem (Ref 8:78). We assume the time dependence of the flux in a multiplying system is given by an exponential growth rate α . Thus,

$$\Phi(\vec{r},E,t) = \Phi(\vec{r},E)\, e^{\alpha t} \tag{3.2}$$

and

$$\Phi(\vec{r}',E',t - \frac{\rho}{v(e)}) = \Phi(\vec{r}',E')\, e^{\alpha t}\, e^{-\frac{\alpha\rho}{v(E)}} \tag{3.3}$$

Substitution of Eqns (3.2) and (3.3) into (3.1) transforms the integral equation into a time independent problem.

A further simplification is made by restricting applications to one-dimensional, spherically symmetric systems. The specialized integral equation is now

$$\Phi(r,E) = \int dV' \frac{e^{-\int_0^{\rho} \Sigma(\rho',E)d\rho'}}{4\pi\rho^2} \int dE'\, \Phi(r',E')$$

$$e^{-\frac{\alpha\rho}{v(E)}}\, \Sigma(r',E')C(r',E')f_{r'}(E'\rightarrow E) \tag{3.4}$$

Note that the time retardation term, $\exp[-\alpha\rho/v(E)]$, can be incorporated into the exponential attenuation term by defining a new cross section

$$\Sigma^*(\rho,E) \equiv \Sigma(\rho,E) + \frac{\alpha}{v(E)} \tag{3.5}$$

We now write the integral equation for one energy group.

$$\lambda\psi(r) = \int dV' \frac{e^{-\int_0^{\rho} \Sigma^*(\rho')d\rho'}}{4\pi\rho^2} \psi(r')\Sigma(r')C(r') \tag{3.6}$$

where

$\psi(r)$ = one group spatial flux distribution

$\Sigma^*(\rho') = \Sigma(\rho') + \frac{\alpha}{v}$

λ = eigenvalue

Equation (3.6) represents an auxiliary problem which is an eigenvalue problem. It can be solved numerically, such as by the power method (Ref 7:291), for the spatial flux distribution $\psi(r)$. In addition, the lowest order eigenvalue of Eqn (3.6) can be made equal to unity (i.e., an exactly critical system) by iterative adjustments to Σ^* as per Eqn (3.5). When the eigenvalue is made equal to one, Eqn (3.5) can be solved for the one group multiplication rate, α.

However, Eqn (3.6) has an infinite number of solutions corresponding to higher order eigenvalues and associated eigenfunctions. There will be a lowest λ, called λ_1, for which the eigenfunction ψ_1 is everywhere positive. The eigenfunctions corresponding to higher order values of λ (λ_n being associated with ψ_n) will have one or more nodal points. In other words, the neutron density will be positive in some regions and negative in others. Feynman (Ref 8:8) interprets negative neutron densities as deficiencies below some positive neutron density. He further states that physical reasoning can be used in interpreting the integral equation if negative neutrons are thought of as actual particles whose presence in a region can cancel the presence of an equal number of positive neutrons. Clearly, increasing the number of nodal points in ψ will decrease the overall significance or contribution from that ψ_n. This is so because leakage of neutrons of opposite sign into one another will become more rapid as the eigenfunction oscillates more rapidly.

It should be noted here that the eigenfunctions, ψ_n, are not mutually orthogonal since the kernel of Eqn (3.6) is not symmetric. Furthermore, there is no guarantee that the functions ψ_n form a complete set, even though this is certainly true for cases of physical interest (Ref 8). But as Kaplan (Ref 12) argues, "completeness is academic and orthogonality is only a minor convenience." This is

especially true for the case of an approximate, numerical solution. Indeed, at most only a few of the set of trial eigenfunctions will be used in the final solution. The only criterion, then, for these eigenfunctions is the "goodness" of the final approximation, i.e., the accuracy of the final solution.

We now turn our attention to the energy dependence of the neutron transport equation. The next goal is to develop an energy integral equation that is analogous to the spatial integral equation.

Energy Integral Equation

An analogous energy integral equation can also be derived from Eqn (3.4). The procedure is to assume spatially invariant material properties and a system of infinite extent. These assumptions allow the spatial integrations of Eqn (3.4) to be performed analytically resulting in Eqn (3.11). However, the development of the energy integral equation presented below is based on conversation of neutrons and serves to give a better physical interpretation of the energy equation.

Let $n(E)$ be the energy dependent neutron number density in units of neutrons per unit volume per unit energy. Then the time rate of change of the neutron number density is just equal to the gains minus the losses. That is,

$$\frac{\partial n(E)}{\partial t} = \text{gains} - \text{losses} \tag{3.7}$$

We assume a system of infinite extent with a spatially constant flux. The contribution of $n(E)$, summed for each energy bin dE', is given by

$$\text{gains} = \int dE' \, n(E')v(E')\Sigma(E')C(E')f(E' \rightarrow E) \tag{3.8}$$

where

$n(E')$ = neutron number density at energy E'

$v(E')$ = neutron speed at energy E'

$\Sigma(E')$ = macroscopic total cross section at energy E'

$C(E')$ = average number of secondary neutrons emitted when a neutron of energy E' undergoes a collision

$f(E' \rightarrow E)$ = probability that a neutron entering a collision with energy E' will emerge with energy E.

Equation (3.8) is nearly self-explanatory. The number density times the speed is just neutron flux. The product

of flux and cross section is the reaction rate. For each reaction there are $C(E')$ neutrons emitted with energy distribution given by $f(E' \rightarrow E)$. In order to obtain the entire gain to $n(E)$, we simply sum or integrate over all energies E' .

The losses term in Eqn (3.7) is even more straightforward than the gains. Since we have assumed an infinite system, there is no leakage. The only loss is due to reactions or collisions that occur at energy E . This is simply the product of flux and total cross section.

$$\text{losses} = n(E)\, v(E)\, \quad (E) \tag{3.9}$$

Equation (3.7) can now be written as

$$\frac{\partial n(E)}{\partial t} = \int dE'\, n(E')\, v(E')\, \Sigma(E')\, C(E')\, f(E' \rightarrow E)$$

$$- \; n(E)\, v(E)\, \quad (E) \tag{3.10}$$

But again, as in Eqn (3.2), we claim to know the time dependence of our system. In this case, the exponential growth rate is given by α_∞ since we have assumed an infinite system. Taking the partial derivative in Eqn (3.10) and rearranging, we have the energy integral equation.

$$[\alpha_\infty + v(E)\Sigma(E)]\, n(E) =$$

$$\int dE'\, n(E')v(E')\Sigma(E')C(E')f(E'\rightarrow E) \qquad (3.11)$$

Note that Eqn (3.11) is another eignevalue problem. The lowest order solution $n_1(E)$, corresponds to the energy distribution in a homogeneous, infinite medium. Just as in the spatial case, there are an infinite number of solutions corresponding to higher order eigenvalues and associated eigenfunctions. The lowest order solution, $n_1(E)$, will be everywhere positive and higher order eigenfunctions will have one or more nodal points. The energy eigenfunctions are also not mutually orthogonal, although the adjoint or left eigenfunctions are orthogonal to the right eigenfunctions. Completeness of the energy set of functions is again academic since at most only a few eigenfunctions will be used to approximate the final solution.

We now have methods for determining the spatial flux independent of energy, and also for determining the energy distribution independent of spatial location. The next step is to combine or synthesize the solutions to the separated problem. The final solution, a judicious combination of the separate solutions, will be the integral equation synthesis approximation to the two dimensional, i.e., space and energy, non-separable problem.

Synthesis of Spatial and Energy Solutions

Assuming the spatial and energy eigenfunctions form a complete set, the neutron flux can be expanded in terms of these trial eigenfunctions:

$$\Phi(r,E) = \sum_i \sum_j a_{ij} \psi_i(r) n_j(E) \qquad (3.12)$$

Since the sets of spatial and energy trial functions are known, a good approximation to the flux should be available once a few of the expansion coefficienct, a_{ij}, are obtained.

In order to simplify the bookkeeping notations, we arrange the trial solutions in an arbitrary but consistent order so that trial solution number one is $\psi_1(r) n_1(E)$, trial solution number two is $\psi_2(r) n_1(E)$, trial solution number three is $\psi_i(r) n_2(E)$, trial solution four is $\psi_2(r) n_2(E)$, etc.

The standard methods of perturbation theory (Ref 14:413) are used to obtain the expansion coefficients. That is, we first operate on the trial solution with the exact, two-dimensional kernel of Eqn (3.4). In other words, replace $\Phi(r',E')$ on the right hand side of Eqn (3.4) with the known $\psi_1(r') n_1(E')$. It is important to note that Eqn (3.4) is no longer an eigenvalue problem; it simply represents an integration that must be performed to obtain the flux $\Phi(r,E)$. This integration can be performed

numerically quite quickly since no iteration or simultaneous solutions to equations are required.

Let the result of the integration be $X_1(r,E)$, the subscript denoting that the first trial solution was used on the right hand side of Eqn (3.4). We can then use adjoint weighting to expand $X_1(r,E)$ in terms of all the trial eigenfunctions $\psi_i\, n_j$ and let the expansion coefficients by A_{1n}. The first subscript on A denotes that X_1 is being expanded and the second subscript identifies the coefficient as belonging to the n^{th} trial solution. That is,

$$X_1(r,E) = \sum_{n=1}^{N_{max}} A_{1n}\, \psi_i\, n_j \qquad i,j = 1,2,... \tag{3.13}$$

and clearly

$$A_{1n} = \frac{\int\int X_1(r,E)\psi_i^\dagger(r)n_j^\dagger(E)\,dr\,dE}{\int\int \psi_i^\dagger\, \psi_i\, n_j^\dagger\, n_j\, dr\,dE} \tag{3.14}$$

where the dagger terms are the left or adjoint eigenfunctions found from Eqn (3.6) for spatial functions and from Eqn (3.11) for energy functions. The denominator in Eqn (3.14) can easily be made unity with proper normalization of the separate eigenfunctions.

Similarly, the integration indicated in Eqn (3.4) is performed after substituting $\psi_2 n_1$, $\psi_1 n_2$, $\psi_2 n_2$, etc. for $\Phi(r',E')$ on the right hand side of Eqn (3.4). The results of these integrations are labelled X_2 , X_3 , X_4 , respectively, and these in turn are expanded in terms of the $\psi_i n_j$ basis set. The expansion coefficients, defined by Eqn (3.14), form a transformation matrix $[A_{mn}]$. This matrix transforms from the $\psi_i(r)\, n_j(E)$ basis to the $X(r,E)$ basis.

Note that, if the trial eigenfunctions $\psi_i\, n_j$ were exact eigenfunctions of the kernel of Eqn (3.4), i.e., of the fully two-dimensional, non-separated kernel, then the matrix $[A_{mn}]$ would be the identity matrix. Thus, the magnitude of the off-diagonal elements of $[A_{mn}]$ give a measure of the validity of the separability assumptions used to obtain Eqns (3.6) and (3.11). In addition, if the choice of trial eigenfunctions is reasonably accurate, then the magnitude of the off-diagonal elements should decrease the further one goes away from the main diagonal.

The next step in the synthesis of the spatial and energy solutions is to use the power method (Ref 7:291) to obtain the largest eigenvalue and associated eigenvector of the transformation matrix $[A_{mn}]$. The elements of the lowest order eigenvector are just the expansion coefficients a_{ij} that we seek for Eqn (3.12).

Now that a new and much more accurate approximation to the flux is available through Eqn (3.12), we can use this flux one more time in Eqn (3.4) to perform the right hand side integration. This final integration will yield a more accurate eigenvalue which can then be used to compute the final growth rate, α . We then have solved for the flux as a function of radius and of energy, and have also determined the growth rate for the system.

As pointed out in Section I, the objective of this research was to develop an efficient numerical technique for computing neutron flux and growth rate in specialized systems. However, the entire development in this section has been in terms of continuous functions and continuous variables which are obviously not suitable for direct transfer to digital computers. The computer encoding, numerical techniques and approximations are certainly not a trivial portion of any solution algorithm. Indeed, in the case of integral equation synthesis, a large part of the numerical efficiency can be attributed to a new and unique method of volume integration on a sphere (Ref 17). However, the particular numerical methods remain secondary to the essential ideas of integral equation synthesis. The development and description of numerical techniques used in integral equation synthesis can be found in Appendix A.

In the next section, integral equation synthesis is used to obtain neutron flux and growth rate for small, spherical systems. These results are compared to those obtainable with more conventional (and expensive) calculational schemes.

IV. Results and Discussion

The integral equation synthesis (IES) approach was converted into a Fortran computer program by the author and used to compute the neutron flux and growth rate in some simple systems. In this section the sample problems are described, as well as the results obtainable with this method.

Jezebel Calculations

Jezebel is a bare plutonium sphere, measured to be just critical with a mass of 16.6 kg at a density of 15.8 g/cm^3, corresponding to a radius of 6.4 cm. The isotropic composition of the plutonium is 94.1 wt % Pu-239, 4.8 wt % Pu-240, and 1.0 wt % gallium (Ref 5).

The benchmark for IES calculations is the experimental data reported in LA-3529 (Ref 5). In addition, flux and energy distributions were obtained with the 1977 version of the Los Alamos DTK code using their standard 13 energy group cross section set. The results from the DTK code differ insignificantly from those quoted in LA-3529, and so these sources are used interchangeably as a benchmark and are herein referred to as LASL results.

Cross Sections Used in Calculations

The cross sections used in the IES calculations were a 16 group set collapsed from the 175 group set reported

in UCRL-50400 Vol. 16 (Ref 18). The collapsing was done by Dr. Walt Webster of Lawrence Livermore Laboratory (LLL) who used a group structure and weighting spectrum commonly used at LLL for small, fast, critical assemblies. The group structure and associated group velocities are described in Appendix B.

It is important to note here that the cross sections used in the IES calculation are not identical to those used in the benchmark calculation. This selection was made for two reasons. First, the LLL cross sections were readily available and in a form easily incorporated into the IES methodology. Secondly, and more importantly, it was decided early in this project that the level of accuracy desired with the IES method was inconsistent with highly refined, normalized cross section sets that give good results in only one specific application. Indeed, the authors of the benchmark calculation point out that cross section users often find that normalization is essential to achieve the accuracy required of their calculations (Ref 11). The results reported for the IES calculations are typical of those obtainable with any reasonable cross section set.

Numerical Details

To perform the integrations needed in the integral equation synthesis method, Gaussian quadratures are used for the angular integrations. The Gaussian weights and abscissas are given in Appendix B.

The spatial mesh used in the IES Jezebel calculation consists of a center ball and 17 shells of increasing thickness. For ease of calculation and numerical integration, a self-similar mesh is chosen such that the outside radius of any shell is given by

$$r_i = \varepsilon\, r_{i-1} \tag{4.1}$$

where

r_i = outside radius of an arbitrary shell

r_{i-1} = outside radius of next inner shell

ε = 1.1571

Growth Rate Results

Integral equation synthesis computed the Jezebel alpha to be + 0.39 generations per microsecond, compared to the benchmark value of - 0.65 generations per microsecond. A better appreciation of the accuracy of the IES result can be obtained by converting the alpha values (which should be exactly zero for a critical assembly) to multiplication factor, k (which is exactly one for a critical assembly). The LASL value corresponds to a k of 0.99992 whereas the IES alpha corresponds to a k of 1.00005. This deviation of less than 0.01% is

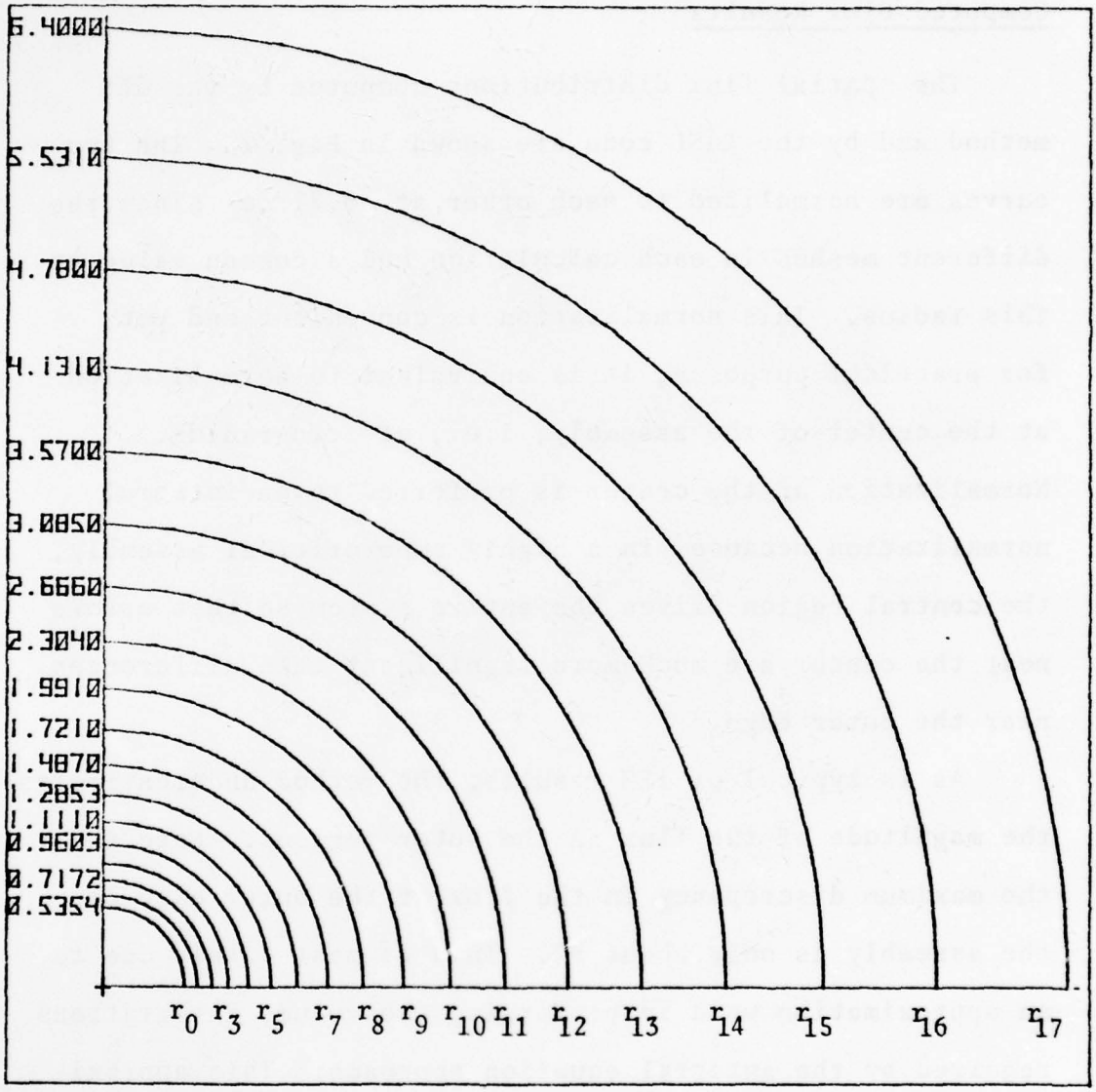

Figure 1. Self-Similar Mesh Used for Jezebel Calculation

indeed negligible in view of uncertainties associated with cross sections and other material properties such as isotopic composition and density.

Computed Flux Results

The spatial flux distributions computed by the IES method and by the LASL code are shown in Fig. 2. The two curves are normalized to each other at 0.71 cm since the different meshes in each calculation had a common value at this radius. This normalization is convenient and yet, for practical purposes, it is equivalent to normalization at the center of the assembly; i.e., at zero radius. Normalization at the center is preferred to an integral normalization because, in a highly supercritical assembly, the central region drives the entire system so that errors near the center are much more significant than differences near the outer edge.

As is typical of IES results, the method underestimates the magnitude of the flux in the outer regions. Note that the maximum discrepancy in the flux at the outer edge of the assembly is only about 8%. This is most likely due to an approximation used in performing the volume integrations required by the integral equation approach. This approximation is not essential to the method, but does significantly reduce the calculational effort. See Appendix A for a detailed description of the geodesic coefficients used in volume integrations.

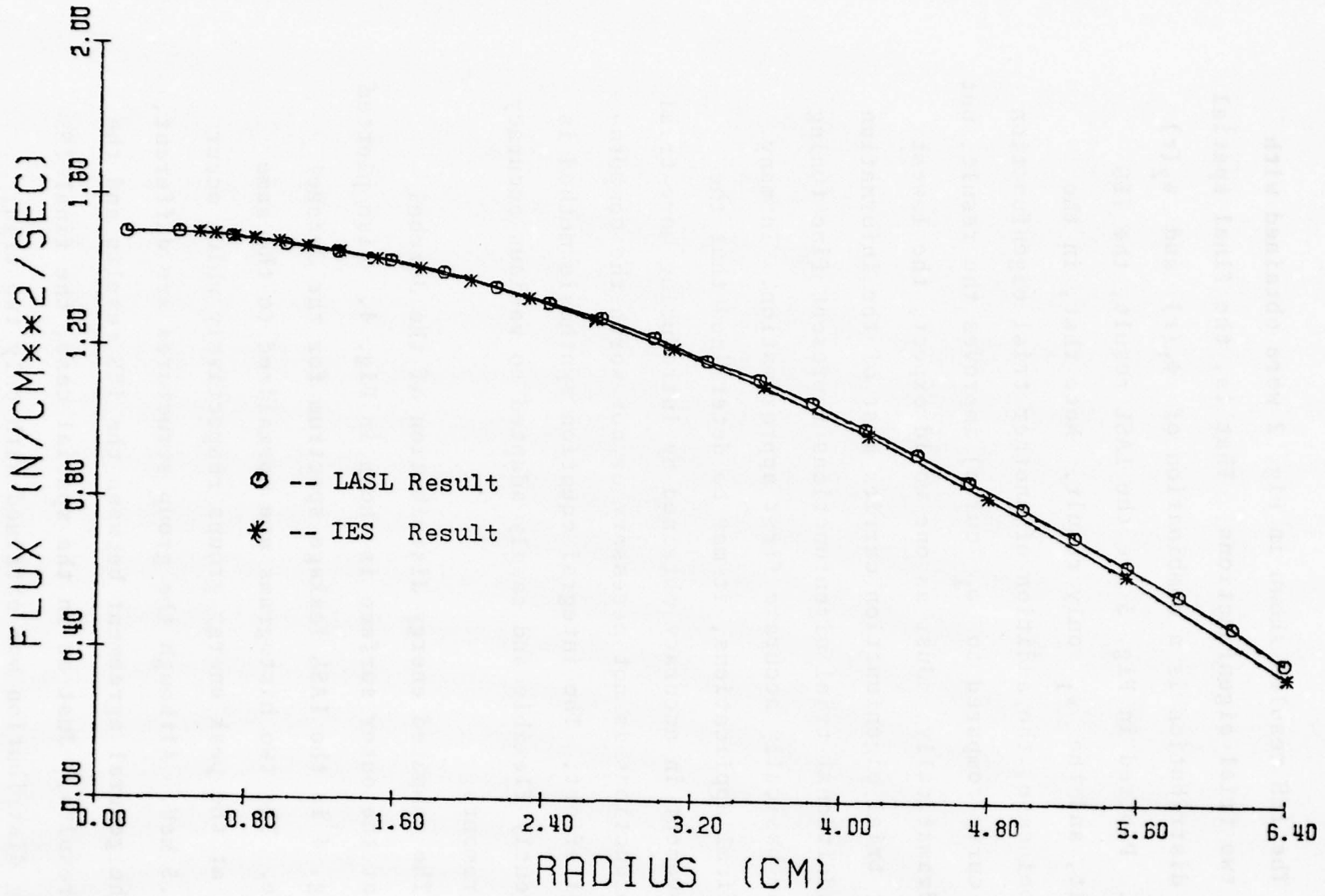

Figure 2. Spatial Flux Distribution for Jezebel Assembly as Calculated by the LASL Code and IES Method

The IES results shown in Fig. 2 were obtained with only two trial eigenfunctions. That is, the final spatial flux distribution is a combination of $\psi_1(r)$ and $\psi_2(r)$ only. Plotted in Fig. 3 are the LASL result, the IES result, and the ψ_1 only result. Note that, in the Jezebel case, the addition of another trial eigenfunction (IES curve compared to ψ_1 curve) improves the result, but not dramatically. Just as one would expect, the lowest order trial eigenfunction carries most of the information and additional trial eigenfunctions represent fine tuning of the basically accurate first approximation. In many practical applications, it may be determined that the improvement in accuracy obtained by introducing more trial eigenfunctions is not necessary or not worth the computational effort. The integral equation synthesis method is inherently flexible and easily adapted to various accuracy requirements.

The computed energy distribution of the Jezebel flux at the outer surface is shown in Fig. 4. Also plotted in Fig. 4 is the LASL leakage spectrum for the Jezebel device. The two histograms are normalized to the same value at the peak energy groups respectively which occur near .5 MeV. Although the group structures are different, not the general agreement between the IES results and the LASL results. Just as in the spatial case, the final IES energy distribution was obtained with only two trial eigenfunctions, $n_1(E)$ and $n_2(E)$. But contrary to the

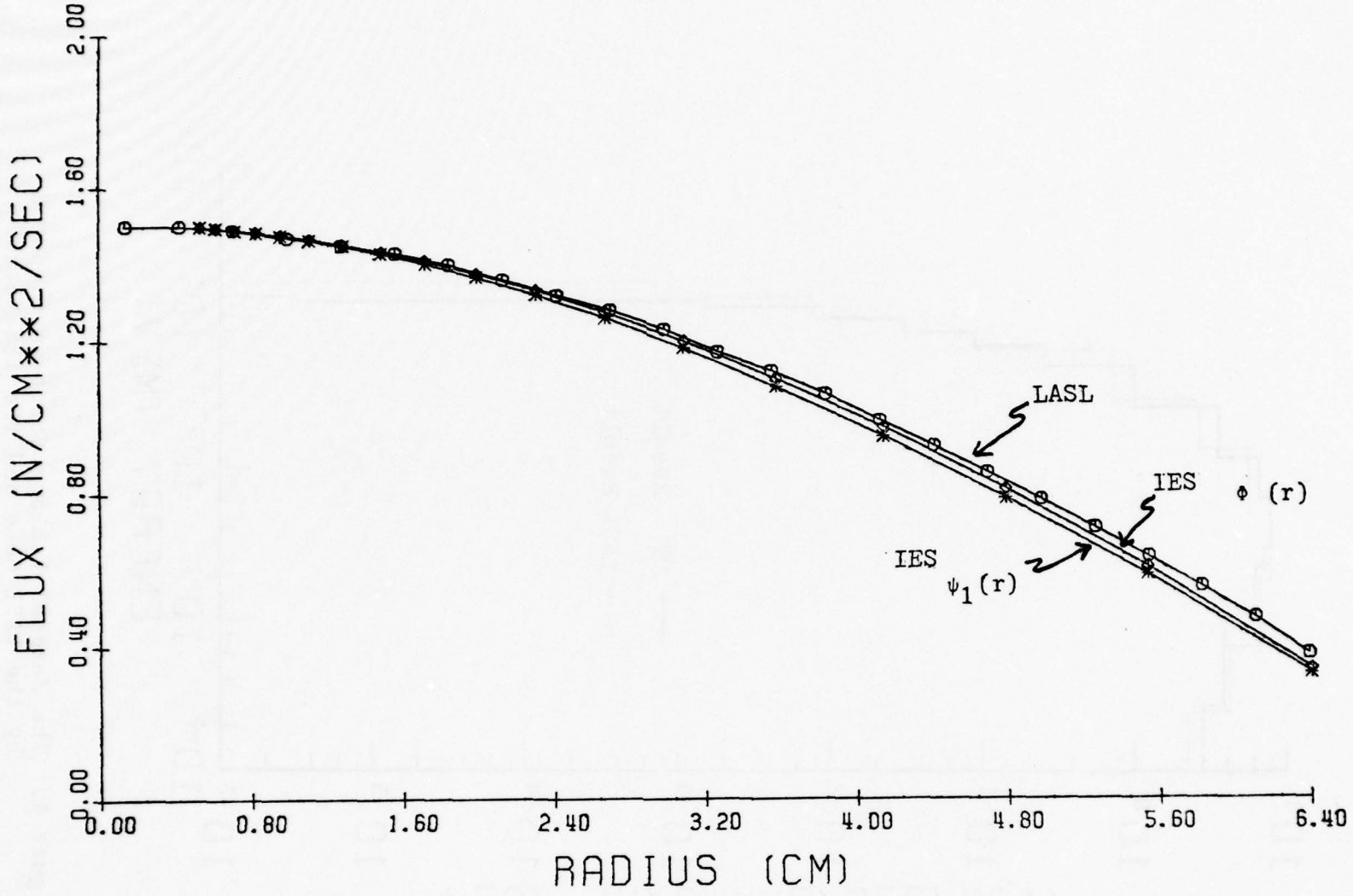

Figure 3. Effect of Additional Trial Eigenfunction on the Jezebel Spatial Flux Distribution

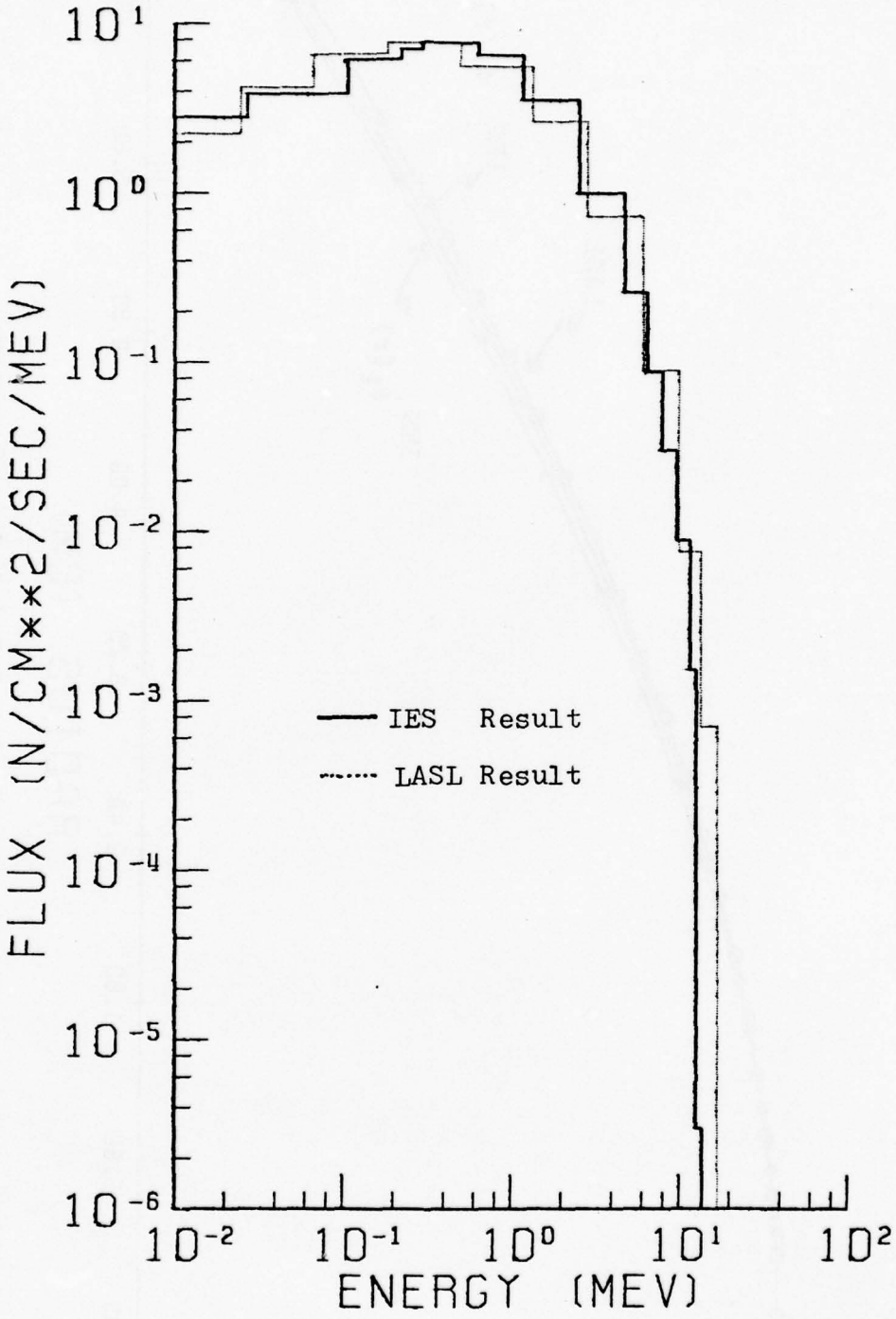

Figure 4. The Jezebel Leakage Spectrum Computed by the LASL Code and the IES Method

spatial case, the addition of the second energy eigenfunction made only negligible changes in the computed spectrum. Obviously, the infinite medium spectrum is very close to the Jezebel spectrum. In other words, essentially all the spectral information is carried in the lowest order trial eigenfunction. We would not expect such a fortuitous computation of energy eigenfunctions in systems of variable density or non-homogeneous composition. In any event, when additional energy eigenfunctions do not significantly alter the final spectrum, it is clearly uneconomical and unnecessary to include more than one trial function.

Shown below in Table I is the transformation matrix computed for the Jezebel system. Note that the terms of maximum magnitude occur on the main diagonal.

Table I
Transformation Matrix from Jezebel Calculation

	$\psi_1 n_1$	$\psi_2 n_1$	$\psi_1 n_2$	$\psi_2 n_2$
X_1	1.0358	-0.0062	0.0019	-0.0004
X_2	-0.0035	0.5728	-0.0003	-0.0015
X_3	0.1891	-0.0011	-0.6621	-0.0218
X_4	-0.0006	0.1059	-0.0156	-0.5149

In Table II below are the expansion coefficients computed from the transformation matrix shown in Table I. Clearly, the maximum information is "contained" in the lowest approximation; i.e., in $\psi_1 n_1$. It is also clear from the relative magnitude of the coefficients shown in Table II that n_2 carries little information. In comparison the second spatial trial function, ψ_2 , contributes about 10% to the final solution.

Table II
Mixing Coefficients for Jezebel Flux Synthesis

Function	Coefficient
$\psi_1 n_1$	0.9938
$\psi_2 n_1$	0.1107
$\psi_1 n_2$	-0.0076
$\psi_2 n_2$	-0.0020

Computation Times

A Fortran program using the IES method has been executed on an IBM 360/75 digital computer. As with all calculations of this type, central processing unit (CPU) times are very problem dependent. The Jezebel calculation

with 17 spatial shells, 16 energy groups, and 4 trial eigenfunctions (2 spatial and 2 energy) requires about 90 seconds CPU time. The same problem with 17 spatial shells, 4 energy groups, and only the lowest order spatial and energy eigenfunctions requires about 10 seconds CPU time.

In comparison, ANISN (an anisotropic, discrete ordinates transport code designed for reactor analysis) requires about five minutes of CPU time on a CDC 7600 computer (Ref 22). Other very sophisticated codes used at LLL to treat small systems require about ten minutes of CDC 7600 CPU time to compute the Jezebel flux and growth rate (Ref 22).

Supercritical and Non-Homogeneous Systems

Integral equation synthesis has been used to calculate various supercritical systems including single-material, variable-density assemblies and also several-material, variable-density systems. Unfortunately, it is difficult if not impossible to find benchmark calculations of this type in the open literature. Yet it is just these more sophisticated systems that integral equation synthesis is designed to calculate.

A validation of a portion of the IES method has been made by solving a one group, supercritical system by several methods. A hypothetical assembly consisting of a 5 cm, double density, bare, plutonium sphere was analyzed

using diffusion theory, a P-1 model, discrete ordinates, the end-point method, and the spatial part of the integral equation synthesis method. Table III shows the computed values for the growth rate α, and the corresponding multiplication factor, k (Ref 3).

Table III
Comparison of Calculated Alpha Values

Model	Alpha (Sec^{-1})	k
Diffusion	2.424×10^8	1.67
P-1	2.727×10^8	1.82
Discrete Ordinates	2.973×10^8	1.96
End-Point	2.965×10^8	1.96
Integral Equation Synthesis	2.987×10^8	1.97

For this problem the end-point method can be considered as nearly exact (Ref 2:96) and hence serves as the benchmark. Notice that diffusion theory predicts an α that differs by 18% from the end-point method. Integral equation synthesis, on the other hand, predicts an α within 0.07% of the end-point value.

Integral equation synthesis has also been applied to multi-material, variable density, supercritical systems. Benchmark results are not available for these assemblies;

however, it is anticipated that the accuracy of the IES results would be consistent with the accuracies indicated above.

V. CONCLUSIONS AND RECOMMENDATIONS

Conclusions

Integral equation synthesis has been shown to be an accurate and efficient technique for calculating neutron flux and growth rate in spherical systems. Because an integral approach is used, the numerical technique does not suffer from convergence problems so common with finite difference schemes. Because the trial functions are computed for each problem, the method does not suffer from the occasional anomalous results of usual synthesis methods (Ref 15) where the trial functions are chosen a priori. And, because the method uses an integral approach, the boundary conditions are automatically and rigorously satisfied (Ref 10).

The computational efficiency of the integral synthesis method arises not only from the method itself, but also from the coarser mesh that can be used in most applications. The use of a self-similar mesh not only simplifies the calculations, but also serves to give maximum spatial resolution of the flux near the center of the system. It is precisely this region that drives the entire assembly so that the fine resolution is well-placed. On the other hand, the regions near the outside edge of a highly supercritical assembly contribute little to the center flux and overall growth rate. The self-similar mesh is

justifiably very coarse near the outer edge of the system.

The mixing coefficients or the actual synthesis of the separate space and energy solutions has been shown to be unnecessary for acceptable accuracy in Jezebel calculations. Clearly, the synthesis procedure is not necessary in problems that are nearly separable in terms of space and energy. Fortunately, the method itself gives an indication of the accuracy of the separability assumption. The transformation matrix, whose lowest order eigenvector produces the mixing coefficients, provides a measure of the separability through the magnitude of the off-diagonal elements. If these elements are large, say within an order of magnitude of the diagonal elements, then the synthesis procedure is probably required because of non-separability. However, if the synthesis procedure is not necessary, the integral method is an even more efficient technique for computing neutron flux in small, supercritical systems. A unique feature of integral equation synthesis is that an interim calculational produce gives an indication of the accuracy of the final product.

The wide applicability of this transport technique cannot be overemphasized. The method is only slightly more complicated than diffusion theory, yet it handles a much broader range of systems. There are no "size compared to mean free path" restrictions as with diffusion theory. The method is applicable to multi-material systems with

varying densities and/or systems with center voids. Yet the method accounts for the nonlocal nature of neutron interactions in a multiplying system. The applicability of integral equation synthesis is further enhanced because of its modest computing cost in terms of storage and CPU time.

Recommendations

Two extensions of this research and integral equation synthesis are recommended. First, the method should be extended to allow anisotropic scatter and to obtain the angular distribution of the neutrons. As it is well known, the angular distribution of the neutrons can be reproduced from the knowledge of the flux by a simple quadrature (Ref 10). This technique is especially straightforward the the numerical form of the IES method since Gaussian quadrature is already used to perform the angular portion of the volume integrations. Instead of summing the contributions of all angular rays, one has to simply retain and store the contribution of each angular ray. In other words, the angular dependence of the neutron flux is already being computed and all that is required is to retain and extract this information.

Second, integral equation synthesis should be extended to geometries other than spherical. Of course, as it is formulated, the method is independent of geometry. However, the transformation of the theoretical formulation into a

numerical technique has been accomplished only for spherical geometry. Potential applications of this efficient technique will be greatly enhanced when rectangular and cylindrical systems can also be treated.

Bibliography

1. Abramowitz, Milton and Irene A. Stegun, Eds. Handbook of Mathematical Functions with Formulas, Graphs, and Mathematical Tables (Eighth Edition). New York: Dover Publications, Inc., 1965.

2. Bell, George I. and Samuel Glasstone. Nuclear Reactor Theory. New York: Von Nostrand Reinhold Company, 1970.

3. Bigelow, Winfield S. Criticality Analysis of a Highly Supercritical Fissioning Assembly. Paper presented at 1977 American Nuclear Society Student Conference. University of Illinois, April 1977.

4. Cockayne, John Edwin. Improved Fast Reactor Space-Energy Synthesis. Unpublished thesis. Purdue University, January 1970.

5. Cremer, C. C., et. al. Comparison of Calculations with Integral Experiments for Plutonium and Uranium Critical Assemblies. LAMS-3529, Los Alamos Scientific Laboratory, October 1969.

6. Davison, B. Neutron Transport Theory. London: Oxford University Press, Amen House, 1958.

7. Faddeev, D. K. and V. N. Faddeeva. Computational Methods of Linear Algebra. San Francisco: W. H. Freeman and Company, 1963.

8. Feynman, R. P. and T. A. Welton. The Calculation of Critical Masses Including the Effects of the Distribution of Neutron Energies. LA-524, Los Alamos Scientific Laboratory, January 21, 1947.

9. Glasstone, Samuel and Alexander Sesonske. Nuclear Reactor Engineering. New York: Van Nostrand Reinhold Company, 1967.

10. Hembd, H. "The Integral Transform Method for Neutron Transport Problems." Nuclear Science and Engineering, 40: 224-238 (October 1969).

11. Hunter, R. E., et. al. Neutron Cross Sections for ^{239}Pu and ^{240}Pu in the Energy Range 1 keV to 14 Mev. LAMS-3528, Los Alamos Scientific Laboratory, September 1968.

12. Kaplan, S. Advances in Nuclear Science and Technology, Vol. 3, P. Greebler and E. J. Henley, Eds., pp. 233-266. New York: Academic Press, 1966.

13. Lancefield, M. J. "Space-Energy Flux Synthesis in Transport Theory." Nuclear Science and Engineering, 37: 423-442 (May 1969).

14. Merzbacher, Eugen. Quantum Mechanics (Second Edition). New York: John Wiley and Sons, Inc., 1970.

15. Nelson, Paul and Harold D. Meyer. "Convergence Results and Asymptotic Error Estimates for Galerkin-Type Spectral Synthesis." Nuclear Science and Engineering, 64: 638-643 (February 1977).

16. Neuhold, R. J. and K. O. Ott. "Improvements in Fast Reactor Space-Energy Synthesis." Nuclear Science and Engineering, 39: 14-24 (July 1969).

17. Nickel, George. Private Communication.

18. Plechaty, E. F., et. al. Tabular and Graphical Presentation of 175 Neutron Group Constants Derived From the LLL Evaluated Neutron Data Library (ENDI). UCRL-50400, University of California, Livermore, California: Lawrence Livermore Laboratory, April 1, 1976.

19. Serber, R. The Graphical Representation of Critical Masses and Multiplication Rates. LA-234, March 6, 1945.

20. Stacey, Weston M., Jr. "Variational Flux Synthesis Methods for Multigroup Neutron Diffusion Theory." Nuclear Science and Engineering, 47: 449-469 (September 1971).

21. Toivanen, T. "On the Variational and Bubnov-Galerkin Synthesis of the Epithermal, Spatially Dependent Neutron Energy Spectra." Journal of Nuclear Energy, 22: 283 (1968).

22. Webster, Walter. Private Communication.

Appendix A

Numerical Methods Used in the IES Calculations

The integral form of the neutron transport equation for one energy group can be written

$$\psi(r) = dV \frac{e^{-\int_0^{\rho} \Sigma(\vec{r} + \vec{\rho}')d\rho'}}{4\pi\rho^2} \Sigma(\vec{r}')C(\vec{r}')\psi(\vec{r}')\, e^{-\frac{\alpha\rho}{v}} \qquad (A.1)$$

where

$\psi(\vec{r})$ = scalar neutron flux in neut/cm^2-sec

$(\vec{r})$ = space point to be calculated

$(\vec{r}')$ = other space points over which we integrate

ρ = $|\vec{r} - \vec{r}'|$

$\Sigma(r')$ = total macroscopic cross section at $\vec{r}'$

$C(r')$ = average number of neutrons everging from a collision at $\vec{r}'$

v = neutron velocity

α = neutron growth rate

The basic problem is to solve Eqn (A.1) numerically and efficiently for a spherical system. There are many ways in which this can be done; however, the following method is quite efficient.

The first decision involves the geometry of the integration. So far, we have just indicated an integration over dV'. The usual procedure is to define the vectors $\vec{r}$ and $\vec{r}'$ from the center of spherical geometry. By appropriate transformations of the variables, it is possible to arrive at an integral equation whose kernel is symmetric in $\vec{r}$ and $\vec{r}'$. There are several advantages to this approach, particularly in that the solutions to the equation then form an orthogonal set. Also, many matrix manipulation schemes are simpler when the matrix is symmetric. The difficulty, however, is that a discontinuity arises when $\vec{r}' = \vec{r}$. This can be avoided by sacrificing symmetry and using ρ as the variable of integration. We then have

$$dV = 2\pi \sin\theta d\theta \, \rho^2 \, d\rho \tag{A.2}$$

where θ is the angle between $\vec{r}$ and ρ, and the discontinuity is eliminated.

The integral over dV' now involves only two dimensions since the problem is symmetric in azimuthal angle. The integration over θ can be quickly transformed into one over $\mu = \cos\theta$ since

$$\int_0^{\pi} \sin\theta d\theta \, f(\theta) = \int_{-1}^{1} d\mu \, f(\mu) \tag{A.3}$$

Integrals of this type are most accurately approximated by Gaussian quadratures:

$$\int_{-1}^{1} d\mu\ f(\mu) \simeq \sum_{k=1}^{K} \omega_k\ f(\mu_k) \tag{A.4}$$

For each value of K, tables (Ref 1) give the corresponding values of the weights ω_k and the direction cosines μ_k. Using Gaussian quadratures, the entire volume integral now reduces to a weighted sum of K one-dimensional integrals over ρ. Integral equation synthesis solutions using $K = 10$ have been shown to give acceptable convergence of the θ- integration.

$$\psi(r) = \sum_{k=1}^{K} \tfrac{1}{2}\omega_k \int_{o}^{\rho_{max}} d\rho\ e^{-\int_{o}^{\rho} \Sigma^*(\rho')d\rho'}\ \Sigma(r')C(r')\psi(r') \tag{A.5}$$

where

$$\Sigma^* = \Sigma + \frac{\alpha}{v}$$

The final integration over ρ requires some care. We must first define the manner in which known properties (total cross section and average number of neutrons emerging from a collision) and unknown quantities (fluxes) vary as functions of radius. We must then establish a correspondence between

this radial dependence and the dependence on the coordinate ρ . Because each integration ray is oblique to the radius vector, this latter correspondence can become geometrically and numerically quite complicated.

Before describing the radial dependence of the variables, the following indices are introduced:

- k = the label of the angular ray along which we are integrating over ρ .
- i = the label of the spherical shells. These are labelled such that i increases as we go out to larger radii.
- j = the label of the crossing points; i.e., the jth shell intersected as we proceed outward along the kth ray. The point from which we start is $j = 0$.
- ℓ = an "offset" index that is a function of k and j . After crossing j shells as we go outward on the kth ray, we intersect the $(i + \ell)$ shell.
- ℓ' = another "offset" index which is either the same as ℓ (if the kth ray is going inward or is just "glancing" across a shell) or equal to $(\ell + 1)$ if the kth ray is going outward. This index specifies the cross sections to be used in the integration.

An example of these indices and relationships are indicated in Fig. A-1.

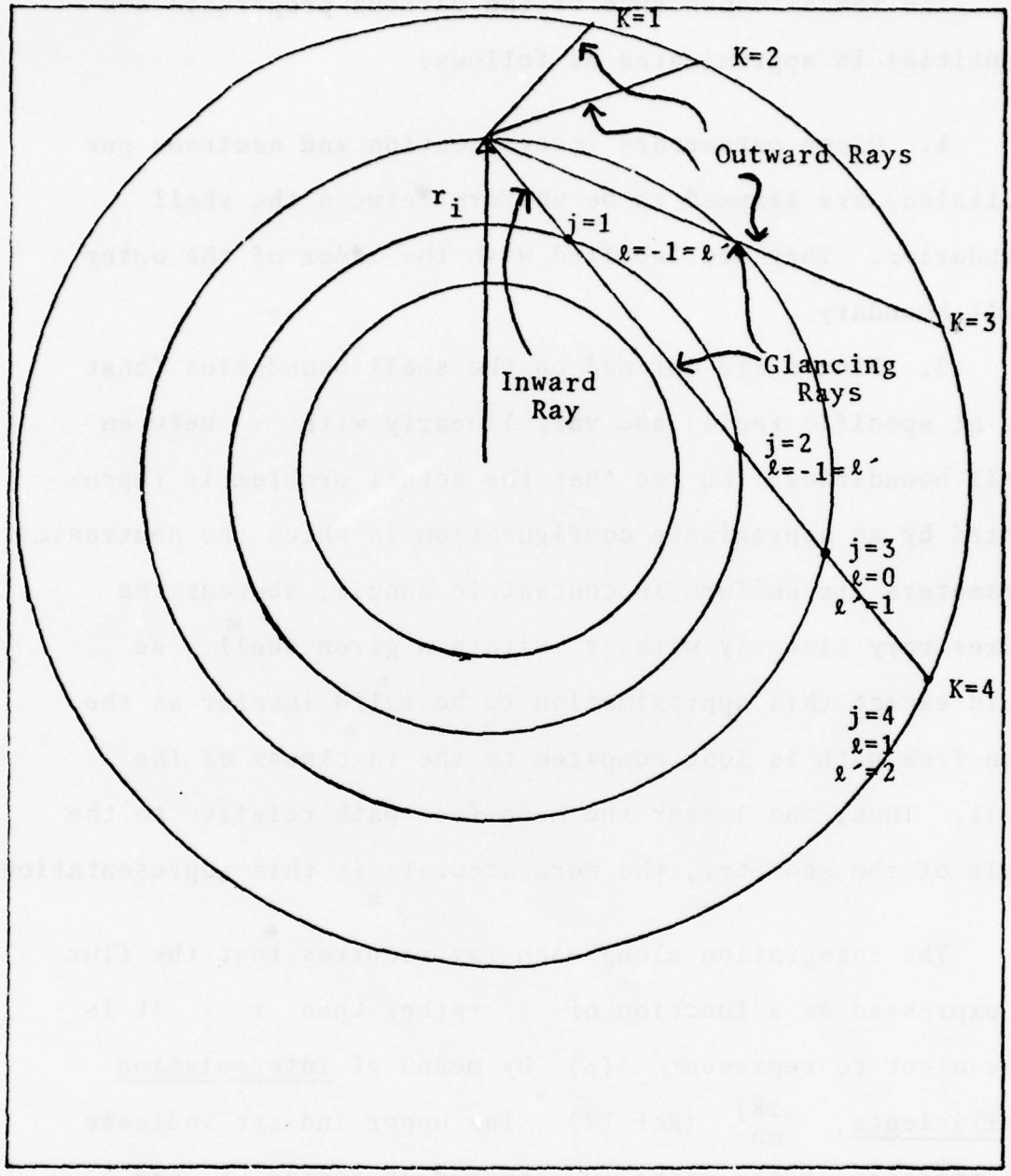

Figure A-1. Several Integration Rays and the Associated Indices.

The radial dependence of the various properties and quantities is approximated as follows:

1. Given parameters (cross section and neutrons per collision) are assumed to be uniform between the shell boundaries. They are labelled with the index of the outer shell boundary.

2. Fluxes are defined on the shell boundaries (that is, at specific radii) and vary linearly with r between shell boundaries. We see that the actual problem is represented by an approximate configuration in which the neutronic parameters are uniform in concentric annuli, whereas the fluxes vary linearly with r within a given shell. We would expect this approximation to be valid insofar as the mean free path is long compared to the thickness of the shell. Thus, the larger the mean free path relative to the scale of the geometry, the more accurate is this representation.

The integration along each ray requires that the flux be expressed as a function of ρ rather than r. It is convenient to represent $\psi(\rho)$ by means of interpolation coefficients, C_{mn}^{ikj} (Ref 17). The upper indices indicate the position in the mesh: we started at radius i and have progressed outward on ray k; this interpolation will apply between boundary crossings j and $j + 1$. The lower indices relate to a polynomial fit involving the values of flux at radii $(i + \ell + m)$, the powers of $(\frac{\rho}{r_i})$ being given by n. These terms are illustrated in Fig. A-2.

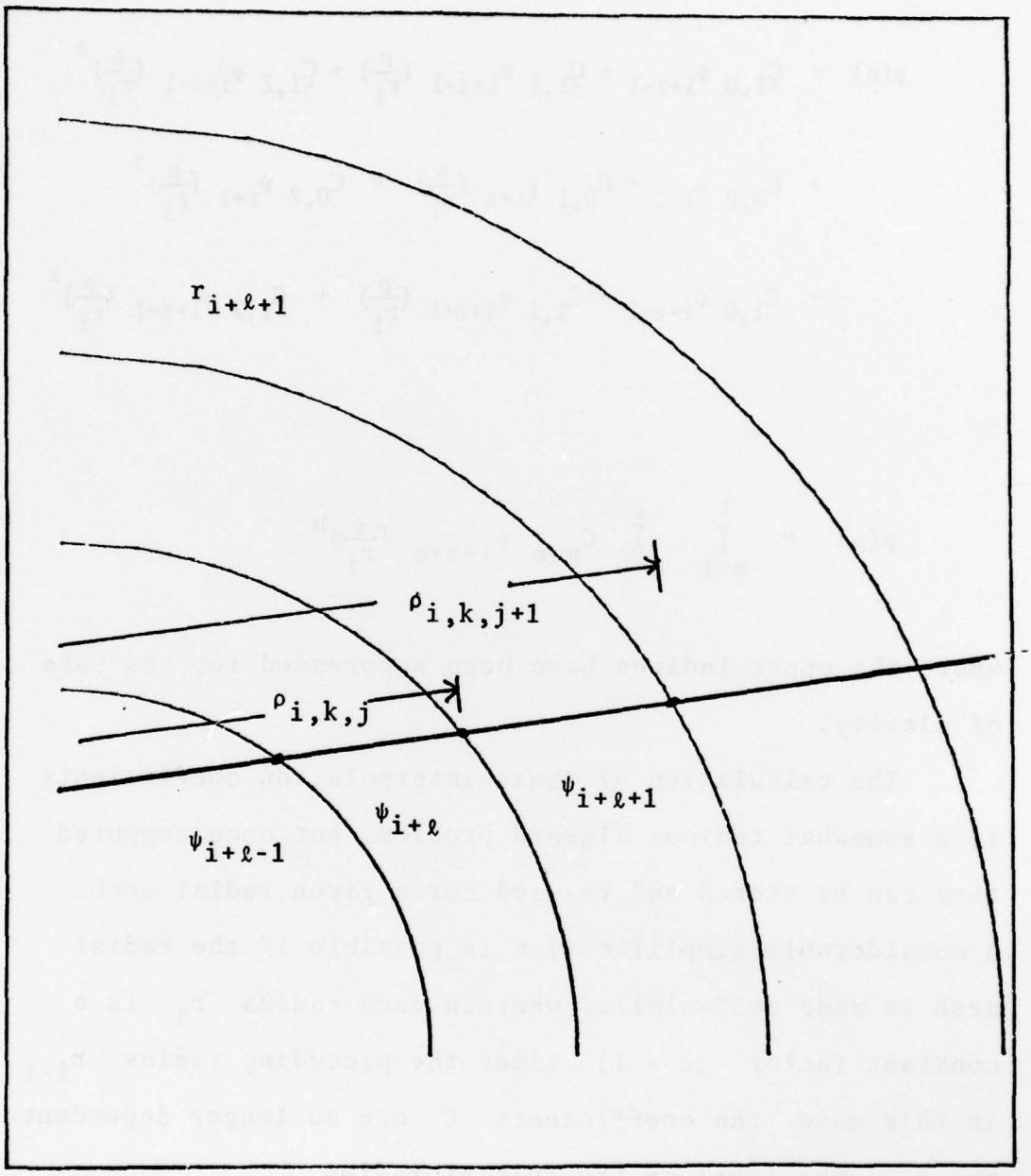

Figure A-2. Relationship of Flux Indices and ρ Indices.

For ρ between ρ_{ikj} and ρ_{ikj+1}, the flux is given by

$$\psi(\rho) = \underline{C}_{1,0}\,\psi_{i+\ell-1} + \underline{C}_{1,1}\,\psi_{i+\ell-1}\left(\frac{\rho}{r_i}\right) + \underline{C}_{1,2}\,\psi_{i+\ell-1}\left(\frac{\rho}{r_i}\right)^2 + C_{0,0}\,\psi_{i+\ell} + C_{0,1}\,\psi_{i+\ell}\left(\frac{\rho}{r_i}\right) + C_{0,2}\,\psi_{i+\ell}\left(\frac{\rho}{r_i}\right)^2 + C_{1,0}\,\psi_{i+\ell+1} + C_{1,1}\,\psi_{i+\ell+1}\left(\frac{\rho}{r_i}\right) + C_{1,2}\,\psi_{i+\ell+1}\left(\frac{\rho}{r_i}\right)^2 \qquad (A.6)$$

or

$$\psi(\rho) = \sum_{m=1}^{1}\sum_{n=0}^{2} C_{m,n}\,\psi_{i+\ell+m}\left(\frac{\rho}{r_i}\right)^n \qquad (A.7)$$

where the upper indices have been suppressed for the sake of clarity.

The calculation of these interpolation coefficients is a somewhat tedious algebra problem, but once computed they can be stored and re-used for a given radial mesh. A considerable simplification is possible if the radial mesh is made self-similar wherein each radius r_i is a constant factor $(\varepsilon > 1)$ times the preceding radius r_{i-1}. In this case, the coefficients C are no longer dependent on i, the label of the initial radius.

The interpolation coefficients are calculated from Eqn (A.7) with the following boundary conditions:

$$@\ \rho = \rho_j \quad ; \quad \psi(\rho) = \psi_{i+\ell} \tag{A.8}$$

$$@\ \rho = \rho_j \quad ; \quad \left.\frac{\partial \psi}{\partial \rho}\right|_{\rho=\rho_j} = \frac{\partial \psi}{\partial r} \frac{\partial r}{\partial \rho} \tag{A.9}$$

$$@\ \rho = \rho_{j+1} \quad ; \quad \psi(\rho) = \psi_{i+\ell+1} \tag{A.10}$$

Note that, depending on the angle of the integration ray k, ρ_{j+1} will be on a shell whose radius is larger than (outward case), the same as (glancing case), or smaller than (inward case) the shell denoted by ρ_j. For this reason, the interpolation coefficients are also divided into outward. glancing, and inward cases. A listing of the interpolation coefficients for a self-similar radial mesh is provided in Table A-1.

At this point, making use of Gaussian quadrature and the interpolation coefficients, we can rewrite Eqn (A.1) as

$$\psi(r) = \sum_{k=1}^{K} \omega_k \sum_{j=0}^{j_{max}} \sum_{m=-1}^{1} \sum_{n=0}^{2} C_{mn}^{jk} \psi_{i'+\ell+m} \Sigma_{i+\ell'} C_{i+\ell'}$$

$$\left\{ \int_{\rho_j}^{\rho_{j+1}} d\rho \left(\frac{\rho}{r_i}\right) e^{-\int_{\rho_j}^{\rho} \Sigma_{i+\ell'} d\rho'} e^{-\frac{\alpha\rho}{v}} \right\} \tag{A.11}$$

The terms above in the brackets are simplified in the following way. Approximate $e^{-\alpha\rho/v}$ as $(1 - \frac{\alpha\rho}{v})$. Define a new variable of integration as

$$y = \frac{\rho - \rho_j}{\rho_{j+1} - \rho_j}$$

Define a transmission factor $T_j^{i,k}$ such that

$$T_{j+1}^{i,k} = T_j^{i,k} \; e^{-\Sigma_{j+1} (\rho_{j+1} - \rho_j)}$$

and

$$T_0^{i,k} = 1$$

Then the bracketed term in Eqn (A.11) can be written as

$$\left\{ \quad \right\} = T_j^{i,k} \int_0^1 dy \; y^n \left[1 - \frac{\alpha}{v} (\Delta\rho y - \rho_j)\right] e^{-\Sigma_{i+\ell} y \Delta\rho} \qquad (A.12)$$

where

$$\Delta\rho \equiv \rho_{j+1} - \rho_j$$

Table A-1

Interpolation Coefficients for A Self-Similar Radial Mesh

M	Case	N=0	N=1	N=2
-1	OUTWARD	0	0	0
	GLANCING	$-\frac{(1-g_{min})x_j x_{j+1}}{\eta_K^2 - x_j x_{j+1}}$	$-\frac{2\eta_K(1-g_{min})}{\eta_K^2 - x_j x_{j+1}}$	$-\frac{(1-g_{min})}{\eta_K^2 - x_j x_{j+1}}$
	INWARD	$g\left(\frac{x_j x_{j+1}}{\Delta x} + \frac{x_j^2}{\Delta x^2}\right)$	$-g\left(\frac{(x_j + x_{j+1})}{\Delta x} - \frac{2x_j}{\Delta x^2}\right)$	$g\left(\frac{1}{\Delta x} + \frac{1}{\Delta x^2}\right)$
0	OUTWARD	$1+g\left(\frac{x_j x_{j+1}}{\Delta x} - \frac{x_j^2}{\Delta x^2}\right)$	$-g\left(\frac{(x_j + x_{j+1})}{\Delta x} + \frac{2x_j}{\Delta x^2}\right)$	$g\left(\frac{1}{\Delta x} - \frac{1}{\Delta x^2}\right)$
	GLANCING	$\frac{K^2 - g_{min} x_j x_{j+1}}{\eta_K^2 - x_j x_{j+1}}$	$\frac{2\eta_K(1-g_{min})}{\eta_K^2 - x_j x_{j+1}}$	$\frac{1 - g_{min}}{\eta_K^2 - x_j x_{j+1}}$
	INWARD	$1-g\left(\frac{x_j x_{j+1}}{\Delta x} - \frac{x_j^2}{\Delta x^2}\right)$	$g\left(\frac{(x_j + x_{j+1})}{\Delta x} + \frac{2x_j}{\Delta x^2}\right)$	$-g\left(\frac{1}{\Delta x} - \frac{1}{\Delta x^2}\right)$
+1	OUTWARD	$-g\left(\frac{x_j x_{j+1}}{\Delta x} + \frac{x_j}{\Delta x^2}\right)$	$g\left(\frac{(x_j + x_{j+1})}{\Delta x} - \frac{2x_j}{\Delta x^2}\right)$	$-g\left(\frac{1}{\Delta x} + \frac{1}{\Delta x^2}\right)$
	GLANCING	0	0	0
	INWARD	0	0	0

Table A-1 (Cont'd)

$\eta_K \equiv \cos\theta$ where θ is the angle between r_i and the kth ray

$x_j \equiv \rho_j / r_i$

$$g' \equiv \frac{x_j + \eta_K}{\frac{r_j}{r_i}(r_{j+1} - r_j)}$$

Then the Table entries are $C_{m,n}^{j,k}$

A second change of variables such that

$$Z = \Sigma_{i+\ell} \Delta\rho \; y$$

allows us to write the bracketed term as

$$\left\{ \right\} = (1 + \frac{\alpha}{v} \rho_j) \left(\frac{1}{b} \right)^{n+1} \int_o^b Z^n e^{-Z} dZ - \left(\frac{\alpha}{v} \Delta\rho \right) \left(\frac{1}{b} \right)^{n+2} \int_o^b Z^{n+1} e^{-Z} dZ \qquad \text{(A.13)}$$

where

$$b \equiv \Sigma_{i+\ell} \Delta\rho$$

But these integrals are just the partial gamma function such that

$$\int_a^b e^{-Z} dZ = e^{-a} - e^{-b} \equiv G_o(a,b)$$

and

$$\int_a^b Z^n e^{-Z} dZ = -b^n e^{-b} + n \int_a^b Z^{n-1} e^{-Z} dZ \qquad \text{(A.14)}$$

or

$$G_n(a,b) \equiv \int_a^b Z^n e^{-Z} dz = -b^n e^{-b} + n G_{n-1}(a,b)$$

Making these substitutions and rearranging, we have the final numerical form of Eqn (A.1):

$$\psi_i = \sum_{k=1}^{K} \sum_{j=0}^{J_{max}} \sum_{m=-1}^{1} \sum_{n=0}^{2} \tfrac{1}{2}\omega_k \Sigma_{i+\ell} C_{i+\ell} T_j^{i,k} C_{m,n}^{j,k}$$

$$\left\{ \frac{G_n(o,b)}{b^{n+1}} - \frac{\alpha}{v} \left[\frac{\Delta\rho}{b^{n+2}} G_{n+1}(o,b) - \frac{\rho_j}{b^{n+1}} G_n(o,b) \right] \right\} \psi_{i+\ell+m} \quad (A.15)$$

Before this equation can be solved numerically, the boundary conditions need to be incorporated. Incorporating the external boundary condition is a trivial matter; the summing over j (the number of shell crossings) continues until the outermost boundary is reached. A simple test of $(i + \ell + m)$ denotes when the outer boundary is reached. The interior boundary condition is a little more complicated. Because of spherical symmetry, the internal boundary condition is

$$\left. \frac{d\psi(r)}{dr} \right|_{r=0} = 0 \quad (A.16)$$

Obviously, a linear variation of flux with radius inside the smallest shell $(r < r_o)$ cannot satisfy the interior boundary condition. For this reason, a quadratic variation of flux with radius is assumed inside r_o. For r less than r_o

$$\psi(r) = A + Br + Cr^2 \tag{A.17}$$

Denoting the flux at the center $\psi(r = 0)$ as ψ_C and applying Eqn (A.16), we have

$$\psi(r < r_o) = \psi_C - \frac{\psi_c - \psi_o}{r_o^2} r^2 \tag{A.18}$$

where $\psi_o = \psi(r_o)$. The center flux ψ_C is computed implicitly as a function of all the ψ_i. That is,

$$\psi_C = \sum_{i=0}^{I_{max}} a_i \psi_i \tag{A.19}$$

where the a_i are obtained from a solution of Eqn (A.1) at $r = 0$. Even though Eqn (A.1) is greatly simplified when $r = 0$, the resulting expansion coefficients a_i are algebraically complicated. They are presented here without derivation.

$$a_o = \frac{C_o}{D} \frac{G_2(\Sigma_o r_{-1}, \Sigma_o r_o)}{r_o^2} + \frac{1}{D} \frac{C_1}{(r_1 - r_o)} [r_1 G_o(\Sigma_1 r_o, \Sigma_1 r_1) T_1$$

$$a_i = \frac{C_i}{(r_i - r_{i-1})} \frac{T_i}{D} [G_1(\Sigma_i r_{i-1}, \Sigma_i r_i) - r_{i-1} G_o(\Sigma_i r_{i-1}, \Sigma_i r_i)]$$

$$+ \frac{T_{i+1} C_{i+1}}{D(r_{i+1} - r_i)} [r_{i+1} G_o(\Sigma_{i+1} r_i, \Sigma_{i+1} r_{i+1})$$

$$- G_1(\Sigma_{i+1} r_i, \Sigma_{i+1} r_{i+1})] \qquad \text{(A.20)}$$

where

$$D = [\frac{1}{C_o} - G_o(\Sigma_o r_{-1}, \Sigma_o r_o) + \frac{1}{r_o^2} G_2(\Sigma_o r_{-1}, \Sigma_o r_1)] C_o$$

$$T_i = \exp[r_{i-1}(\Sigma_i - \Sigma_{i-1})] T_{i-1}$$

$$T_o = 1$$

G_n = partial gamma function as defined in Eqn (A.14)

Having incorporated the boundary conditions, the transformation of Eqn (A.1) to a discretized form is now complete. Clearly, Eqn (A.15) is an eigenvalue problem of the form

$$\lambda \psi_i = \sum_{i'} M_{ii'} \cdot \psi_{i'} \qquad (A.21)$$

It can be solved numerically by techniques such as the power method (Ref 7:291). The procedure is to solve Eqn (A.15) and then adjust α and resolve the equation until the eigenvalue is made equal to unity. The α that makes the system just critical is the one group growth rate that we seek.

Appendix B

Data Listing for Jezebel Calculations

Jezebel calculations were performed with the IES method using a 17 shell self-similar mesh with $r_o = 0.5354$ and $\varepsilon = 1.157129$. The Gaussian quadrature abscissas and weights are listed in Table B-I.

Table B-I
Gaussian Quadrature Abscissas and Weights[a]

Abscissas	0.97391	0.86506	0.67941	0.43340	0.14887
Weights	0.06667	0.14945	0.21908	0.26927	0.29552
Abscissas	-.14887	-.43340	-.67941	-.86506	-.97391
Weights	.29552	0.26927	0.21908	0.14945	0.06667

[a] Data from Ref 1:916.

The sixteen energy groups and their associated average group velocity and cross section used in Jezebel calculations are provided in Table B-II.

Table B-II

Group Structure, Velocities and Cross Sections For Jezebel Calculation[a]

Group	Group Energy Lower Bound (MeV)	Group Velocity (cm/shake)	Transport Cross Section (Barns)
1	13.62[b]	51.60	3.8553
2	12.57	50.24	3.8490
3	11.57	48.19	3.6706
4	9.68	45.24	3.5983
5	7.97	41.00	3.8157
6	6.42	37.01	4.0943
7	4.73	32.48	4.2653
8	2.55	25.68	4.7049
9	1.18	18.26	5.0878
10	0.638	12.91	5.8035
11	0.296	9.263	6.8698
12	0.222	6.988	8.4536
13	0.107	5.373	9.7588
14	0.0273	3.229	11.4430
15	0.00875	1.739	13.9460
16	0.00100	0.7801	16.5620

[a] From Ref 22.

[b] Upper Energy bound on group 1 is 14.60 MeV.

DISTRIBUTION

Organization	No. of Cys
HQ USAF/INET (Lt Col R. W. Ohlwiler) INY (Lt Col D. J. Petersen Washington, DC 20330	1 1
HQ SD/SZJE (Lt Col H. Hayden) P. O. Box 92960 Worldway Postal Center Los Angeles, CA 90009	1
HQ SAC/XPFS (Maj F. P. Tedesco) Offutt AFB, NE 68113	1
AFIT/ENP (Maj G. H. Nickel) Wright Patterson AFB, OH 45433	1
AFWL/DY (Lt Col J. Generosa) (Col T. Ciambrone) Kirtland AFB, NM 87117	1 1
Central Intelligence Agency/NED ATTN: Dr. J. Ingley Washington, DC 20505	1
DARPA/NMRO (Col G. Bulin) 1400 Wilson Blvd Arlington, VA 22209	1
Defense Nuclear Agency Washington, DC 20305	1
Defense Intelligence Agency/DT-1 ATTN: Dr. J. Mansfield Washington, DC 20301	1
Dept of Defense/DOE (Col William Myers) Long Range Planning Group Rm 3E334, Pentagon Bldg Washington, DC 20301	1
AFATL/DLJW (Maj G. Spitale) Eglin AFB, FL 32542	1
Defense Documentation Center/DTIC-TC Cameron Station Alexandria, VA 22314	2

Organization	No. of Cys
Mission Research Corp.	
ATTN: Mr. D. Soule	1
Mr. T. Olds	1
Santa Barbara, CA 93102	
Lawrence Livermore Laboratory	
University of California	
ATTN: Dr. P. C. Giles	1
Dr. J. M. Leblanc	1
Dr. S. F. Eccles	1
Dr. W. M. Webster	1
Technical Director	1
DNA Library	1
P. O. Box 808	
Livermore, CA	
Los Alamos Scientific Laboratory	
ATTN: Dr. D. W. Barr	1
Dr. G. E. Hansen	1
Dr. T. J. Hirons	1
Dr. W. E. Preeg	1
Dr. H. A. Sandmeier	1
Dr. D. R. Worlton	1
P. O. Box 1663	
Los Alamos, NM 87544	
OSD/AE	1
Rm 3E1069, Pentagon Bldg	
Washington, DC 20301	
Research and Development Associates	
ATTN: Mr. E. Martinelli	1
P. O. Box 9695	
Marina Del Rey, CA 90291	
Science Applications, Inc.	
ATTN: Mr. D. K. Hall	1
Dover Road	
Hanover, NH 03103	
Science Applications, Inc.	
ATTN: Dr. J. E. Cockayne	1
8400 Westpark Drive	
McLean, VA 22102	
AFTAC/TR	15
TN	3
TF	1
TA	1